Reprint

VIP *Very Important Paper*

Understanding the Chloride Affinity of Barbiturates for Anion Receptor Design

Andre Nicolai Petelski,*[a, b] Josefina Marquez,[a] Silvana Carina Pamies,[a] Gladis Laura Sosa,[a, b] and Nélida María Peruchena*[b, c]

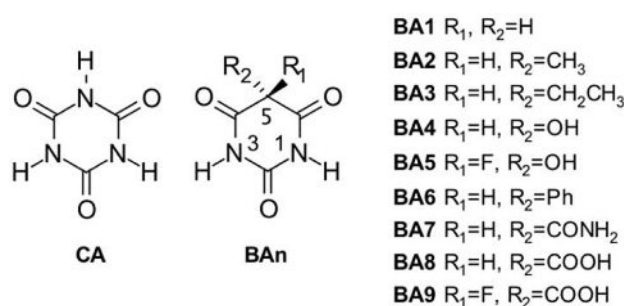*Dedicated to Professor Nélida María Peruchena on the occasion of her 65th birthday*

Due to their potential binding sites, barbituric acid (BA) and its derivatives have been used in metal coordination chemistry. Yet their abilities to recognize anions remain unexplored. In this work, we were able to identify four structural features of barbiturates that are responsible for a certain anion affinity. The set of coordination interactions can be finely tuned with covalent decorations at the methylene group. DFT-D computations at the BLYP-D3(BJ)/aug-cc-pVDZ level of theory show that the C—H bond is as effective as the N—H bond to coordinate chloride. An analysis of the electron charge density at the C—H···Cl⁻ and N—H···Cl⁻ bond critical points elucidates their similarities in covalent character. Our results reveal that the special acidity of the C—H bond shows up when the methylene group moves out of the ring plane and it is mainly governed by the orbital interaction energy. The amide and carboxyl groups are the best choices to coordinate the ion when they act together with the C—H bond. We finally show how can we use this information to rationally improve the recognition capability of a small cage-like complex that is able to coordinate NaCl.

1. Introduction

Within the field of supramolecular chemistry, anion recognition research has gained a notorious interest during the last years.[1–4] In the quest for more efficient anion receptors, several studies have employed the use of hydrogen bonding donor molecules in conjunction with other functional systems, like polysubstituted benzene rings. For instance, squaramides,[5] urea,[6,7] pyrrole,[8] and other nitrogen heterocycle compounds[9] are among the most common building blocks to construct anion receptors.

Certainly, cyanuric acid (CA, see Scheme 1) is, perhaps, one of the most distinguished structure in supramolecular self-assembly. Its molecular structure is so versatile that can be functionalized at its three amine groups. In this context, CA has also been used to design anion receptors. For instance, by alkylation of CA and further organic reactions, Hettche et al.[10]

BA1 R₁, R₂=H
BA2 R₁=H, R₂=CH₃
BA3 R₁=H, R₂=CH₂CH₃
BA4 R₁=H, R₂=OH
BA5 R₁=F, R₂=OH
BA6 R₁=H, R₂=Ph
BA7 R₁=H, R₂=CONH₂
BA8 R₁=H, R₂=COOH
BA9 R₁=F, R₂=COOH

Scheme 1. Molecular structure of cyanuric acid (CA), barbituric acid (BA1) and some derivatives studied herein (BAn, with n = 1–9).

have synthesized an anion host with three conformationally flexible arms. Ravikuma et al.[11] have also exploited this scaffold to build a neutral receptor that selectively traps a sulfate anion within the cavity of the host. Later on, Frontera et al.[12] have investigated the anion-π interactions in CA and some derivatives with an ethyleneammonium arm. They found out that in the co-crystal of the modified systems there is evidence of anion-π and hydrogen bonding between the anions and the host. Mascal et al.[13] went further and synthesized a carcerand-like cage based on two interlinked CA molecules by their triazine N atoms. This CA based cylindrophane was able to selectively trap a fluoride ion via anion-π interactions and hydrogen bonds. In a previous work, we have computationally demonstrated that CA is able to form a hydrogen-bonded quartet with a cage like structure.[14] We also have shown that this complex can also coordinate a sodium chloride ion pair within its cavity through C=O···Na⁺ and π···Cl⁻ interactions. The nature of these interactions goes from electrostatic dominant in

[a] Dr. A. N. Petelski, J. Marquez, S. C. Pamies, Prof. Dr. G. L. Sosa
Departamento de Ingeniería Química
Grupo de Investigación en Química Teórica y Experimental (QUITEX)
Universidad Tecnológica Nacional, Facultad Regional Resistencia
French 414 (H3500CHJ), Resistencia, Chaco, Argentina
E-mail: npetelski@frre.utn.edu.ar

[b] Dr. A. N. Petelski, Prof. Dr. G. L. Sosa, Prof. Dr. N. M. Peruchena
Instituto de Química Básica y Aplicada del Nordeste Argentino
IQUIBA-NEA, UNNE-CONICET
Avenida Libertad 5460, 3400 Corrientes, Argentina
E-mail: arabeshai@yahoo.com.ar

[c] Prof. Dr. N. M. Peruchena
Área de Química Física - Departamento de Química
Laboratorio de Estructura Molecular y Propiedades (LEMyP)
Facultad de Ciencias Exactas y Naturales y Agrimensura
Universidad Nacional del Nordeste
Avenida Libertad 5460, 3400 Corrientes, Argentina

ChemPhysChem

Articles
doi.org/10.1002/cphc.202100008

**Chemistry
Europe**
European Chemical
Societies Publishing

the free state CA@Cl⁻ to orbital dominant in the confined state CA$_4$@Cl⁻. Thus, these contributions demonstrate that this molecule is a potent platform to further obtain anion receptors.

On the other hand, barbituric acid (BA) or 2,4,6-(1H,3H,5H)-pyrimidinetrione (see Scheme 1, BA1) is a similar compound to CA and it has served as a skeleton base for many famous drugs like barbital, a hypnotic medicine. This is because BA acquires pharmacological activity only when it is covalently modified at the methylene group (position 5, see also Scheme 1). The chemistry of this molecule has been reviewed in several opportunities.[15–17] Among this compilations, BA stands out because of its uses in coordination chemistry. It has the ability to form a wide variety of co-crystals. For instance, in the formulation of KBr disks for infra-red measurements, it has been found that pure BA undergoes a co-crystal reaction with the salt by applying only pressure.[18] Furthermore, the N—H and C=O bonds allow BA to form hydrogen-bonded aggregates with almost any organic molecule. In a recent work, Resnati and coworkers[19] have shown that in X-ray structures of 5,5-dihalogenated barbituric acids (X=F, Cl, Br) they form C=O···C-(sp³) tetrel bonds within the lattice structure. Nevertheless, to the best of our knowledge, the capabilities of BA to coordinate anions have not been considered yet.

In the present work, we aim to analyze and tune the chloride affinity of BA and its derivatives. Consequently, we use this information to improve the coordination energy of the CA complex that was studied in ref. [14]. Our results show that BA1 derivatives are superior to CA to recognize anions. The coordination capacity of the methylene group (C5) is as robust as that of the amine group. This coordination can also occur in four distinctive ways, and its strength is distinctly structure and covalent modification dependent. The acidity of BA1 is a key factor for the coordination. We therefore conclude that BA derivatives are potent building blocks for supramolecular anion recognition techniques.

Computational Details

A set of 10 molecular fragments was selected, comprising cyanuric acid (CA) as a reference, barbituric acid (BA1) and eight derivatives covalently modified at position 5, as shown in Scheme 1. All structures were optimized without restriction with dispersion corrected density functional theory (DFT-D) implemented in the Gaussian 09 package,[20] by using the BLYP-D3(BJ) hybrid functional with the aug-cc-pVDZ Dunning basis set. The empirical dispersion correction for the BLYP functional was applied with the IOp 3/124= 40 keyword. This functional has shown a reliable performance in hydrogen bonded systems with similar interactions and in the presence of chloride.[14,21] On the basis of the study of Frontera et al.[12] about anion-π interactions of CA with fluoride, chloride and bromide at the MP2(full)/6-31++G(d,p) level, we also compute their interaction energies by using the ω-B97XD, the M06-2X and the BLYP-D3(BJ) functionals and the MP2 method with the aug-cc-pVDZ basis set. Among them, our chosen method was found to be more adequate to describe this type of interaction (see Table S1). The ω-B97XD and the M06-2X functionals overestimate the interaction energy for chloride. The minimum energy nature of the optimized structures was verified using the vibrational frequency analysis. The bonding energy ΔE_{bond} [Eq. (1)] values were obtained

at the same level of theory calculated as the sum of the interaction energy of the complex ΔE_{int} and the energy needed to deform the isolated structures to the state they acquire in the complex ΔE_{def}. The interaction energies were corrected for the basis set superposition error (BSSE) within the counterpoise procedure of Boys and Bernardi.[22]

$$\Delta E_{bond} = \Delta E_{int} + \Delta E_{def} \tag{1}$$

Geometry optimizations were also carried out in water at the same level of theory by employing the polarizable continuum model (PCM).[23]

The redistribution of the electron density was analyzed within the framework of the quantum theory of atoms in molecules (QTAIM).[24] Total electron densities were calculated at the B3LYP/6-311++G(d,p) level of theory. The local properties at the bond critical points were computed using the AIMALL program.[25]

The interactions were also analyzed with the localized molecular orbital energy decomposition[26] (LMOEDA) method at the BLYP-D3(BJ)/aug-cc-pVDZ level of theory, using the GAMESS quantum chemistry package.[27] This method partitions the interaction energy into four components, according to Equation (2):

$$\Delta E_{int} = \Delta E_{ele} + \Delta E_{ex+rep} + \Delta E_{pol} + \Delta E_{disp} \tag{2}$$

where the term ΔE_{ele} describes the classical electrostatic interaction (Coulomb) of the occupied orbitals of one monomer with those of another monomer; ΔE_{ex+rep} is the attractive exchange component resulting from the Pauli exclusion principle and the interelectronic repulsion; ΔE_{pol} accounts for polarization and charge transfer components; and ΔE_{disp} corresponds to the dispersion term.

Natural Bond Orbital[28] (NBO) analyses were also performed with Gaussian 09 at the BLYP-D3(BJ)/aug-cc-pVDZ. This analysis was conducted to quantitatively evaluate the interactions of charge transfer involved in the formation of C—H···Cl⁻ hydrogen bonds.

2. Results and Discussion

2.1. Acidity of the Methylene Group

Barbituric acid has a pKa of 4.[16,29] The acidity of the methylene group was attributed just to the special arrangement of atoms comparable to that of urea and malonyl esters.[29] Since the endocyclic nitrogen is the second acid group, BA1 can potentially form two coordination complexes, as can be seen in Figure 1a. The coordination strengths are almost equal for both systems, being the C—H···Cl⁻ interaction 1 kcal mol⁻¹ more stabilizing. However, in water, the N—H···Cl⁻ interaction is 3.1 kcal mol⁻¹ more stabilizing than that of the C—H bond. According to the Gibbs free energies of bonding, the thermodynamic preference in gas phase of the N—H···Cl⁻ interaction over the C—H···Cl⁻ one is 6.8 kcal mol⁻¹. The isolated molecule of BA1 is completely planar (Figure 1b, left), but, when chloride interacts with the C—H bond, the methylene group moves out of the ring plane as shown in Figure 1b (right). This structural change has an impact on the shape of the frontier molecular orbital Figure 1c, and it is slightly stabilizing. Therefore, the C—H bond becomes a better partner to interact with chloride. In the
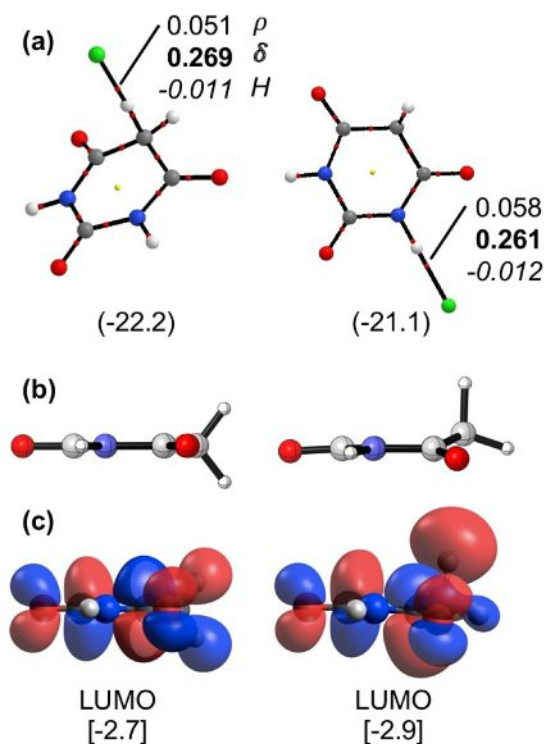
ChemPhysChem

Articles
doi.org/10.1002/cphc.202100008

**Chemistry
Europe**
European Chemical
Societies Publishing

Figure 1. a) Molecular graphs of BA1@Cl⁻ complexes forming a C−H···Cl⁻ hydrogen bond (left) and an N−H···Cl⁻ hydrogen bond (right). Charge density ρ (a.u.) at the bond critical points, delocalization index $\boldsymbol{\delta}$ (a.u.) in bold, total energy density H (a.u.) in italic and bonding energies in parenthesis (kcal mol⁻¹) are shown. b) Side structures of isolated BA (left) and within C−H···Cl⁻ complex (right). c) Lowest Unoccupied Molecular Orbitals (LUMO) and energies (in ev) of isolated BA1 (left) and BA1 upon interaction with chloride via the C−H bond (right).

context of the QTAIM, the delocalization index $\delta(A,B)$ (average number of electron pairs shared between atoms A and B) and the total energy density H (sum of kinetic G and potential energy densities K) are considered descriptors of covalent character.[30,31] In this case, both systems show similar values of $\delta(H,Cl^-)$, negative values of H and positive values of laplacian (Figure 1a, laplacian not shown), indicating that both interactions have a comparable covalent character and consequently similar strengths. With regards to the charge density at the bond critical point, some authors have reported linear relationship between this parameter and the interaction energy,[32,33] but there have also been reports of correlations with the atomic

distances.[34] Herein, we take the bonding energies as a parameter of strength. These results then confirm that the C atom of the methylene group owns a strong capacity to form hydrogen bonds alike the endocyclic N atoms.

Next, we further analyze related compounds to find out whether it is a matter of the structure or if other methylene groups with similar environments can show up the same acidity. Figure 2 displays seven related compounds having a methylene group along with their electrostatic potentials and molecular graphs. Since the QTAIM descriptors are distance dependent, we took the distance and angle parameters of the C−H···Cl⁻ interaction within the optimized complex of BA1@Cl⁻ to constrain all the systems **2** to **7**.

The maximum surface potential values, denoted as $V_{S,max}$, are commonly used to study the trends in some interactions like hydrogen and halogen bonds.[35–37] For instance, the maxima at H atoms of some carboxylic acids have shown good linear correlation with experimental pKa values.[38] As can be seen in Figure 2, the interaction energies show the superior coordinating capacity of barbituric acid **1**. Despite compound **5** has a larger $V_{S,max}$ than BA1 (compound **1**), the later shows the strongest interaction energy. Besides, compound **2** has a $V_{S,max}$ 10.1 kcal mol⁻¹ smaller than in compound **1**, while compounds **3** and **4** show no appreciable $V_{S,max}$. Therefore, it seems that the electrostatic is not the dominant role in these interactions. The charge density at the H···Cl⁻ bond critical points shows no difference among all the complexes (Supporting information Table S2). Then these values demonstrate the incompleteness of this parameter to consider the strength of a bond. On the other hand, the delocalization index and the total energy densities adopt distinctive values and they become less pronounced from complex **2** to **7**. That is, the covalent character decreases from **2** to **7**. Thus, all point towards that the orbital interaction is crucial for the acidity. When looking at the LUMO orbitals of compounds **1**–**7** and their corresponding energies (Figure S1 in the Supporting Information), compounds **1** and **2** show a better symmetry and energy to favorably interact with the HOMO of chloride. These results agree with the trends in Second-Order Perturbation Energies E(2) of Table S3 for compounds **1**, **2** and **3**.

We then performed an energy decomposition analysis on complexes 1@Cl⁻ to 7@Cl⁻ (Table 1). Our analysis indeed show that the predominant component is the orbital interaction, being the largest one for compound **1** and **2**. For example, compound **1** and **5** exhibit the same amount of electrostatic

Table 1. Local molecular orbital energy decomposition analysis (in kcal mol⁻¹) of related compounds of barbituric acid obtained at B3LYP/6-311++G(d,p) level of theory.[a]

Complex	ΔE_{int}	ΔE_{ele}	ΔE_{ex+rep}	ΔE_{pol}	ΔE_{disp}
1@Cl⁻	−27.6	−26.0	43.4	−38.4	−6.7
2@Cl⁻	−19.7	−20.1	44.3	−37.6	−6.3
3@Cl⁻	−22.0	−26.5	45.2	−34.0	−6.7
4@Cl⁻	−10.4	−18.5	45.0	−30.8	−6.2
5@Cl⁻	−13.7	−25.5	47.1	−29.2	−6.2
6@Cl⁻	2.8	−6.1	46.0	−30.8	−6.3
7@Cl⁻	−7.6	−22.4	46.5	−25.3	−6.4

[a] Distances $d(H···Cl^-)$ and angles $\angle C-H···Cl^-$ were constrained at 1.932 Å and 177.2° respectively (see also Figure 2).
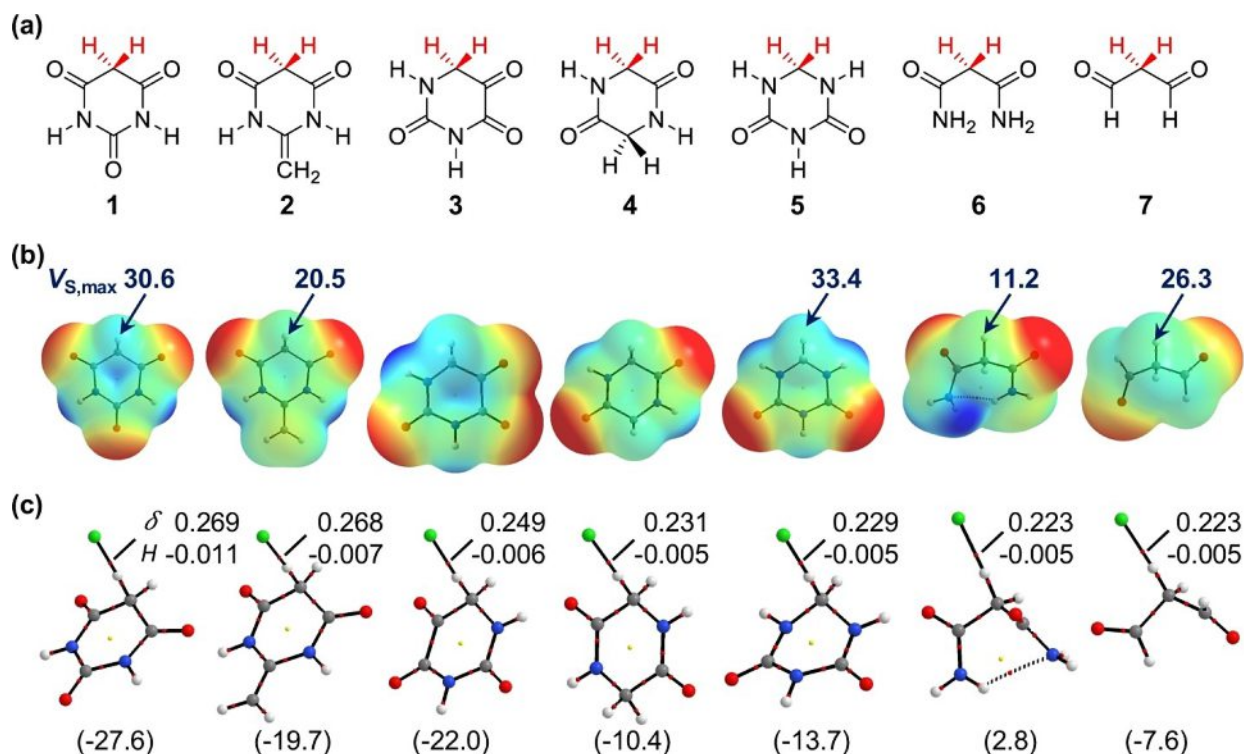
Figure 2. a) Molecular structures of related compounds of barbituric acid **1**. 2-methylenedihydro-4,6(1H,5H)-pyrimidinedione **2**, isobarbituric acid **3**, 2,5-Piperazinedione **4**, 1,3,5-triazinane-2,4-dione **5**, malonamide **6** and 1,3-propanedial **7**. b) Molecular electrostatic potentials of optimized isolated compounds. $V_{S,max}$ values at C–H bonds are indicated in kcal/mol. c) Molecular graphs of C–H···Cl$^-$ systems. δ(H,Cl) and H_b values at H···Cl$^-$ bond critical points are indicated in a.u. Interaction energies in kcal mol^{-1} are indicated in parenthesis.

interaction energies but the orbital + polarization interaction controls the global interaction energy. An NBO analysis on these complexes (Table S3) indicates that the C–H anti-bond in BA1 system experiences the largest population and the lowest energy destabilization. The energy associated to the n→σ* charge transfer is also the greatest one. It is also worth mentioning that, among all the compounds **1** to **7**, only **1**, **2** and **3** are able to form stable complexes with a C–H···Cl$^-$ interaction.

Overall, our results indicate that the orbital interaction plays a key role in the acidity of the methylene group. Despite compounds **1** and **3** share the same number and type of atoms, the former has a coordination energy 5.6 kcal mol^{-1} larger. The electrostatic attraction is equal for both systems but the orbital interaction (and Pauli repulsion to a lesser extent) is the component that makes the difference. Thus, the special arrangement of atoms in BA1 favors the C–H antibond in receiving more charge transfer from chloride.

2.2. Non-Covalent Interactions between Chloride and Barbiturates

We have seen that BA1 has two different anion binding sites. After introducing covalent modifications at position 5, we found out that a chloride anion can interact with the barbiturate through two new specific ways, as shown in Scheme 2. There-
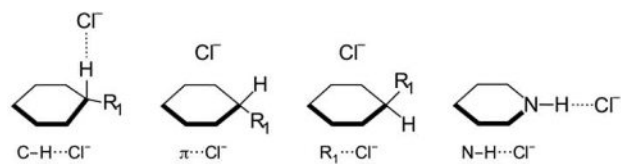
Scheme 2. Schematic representation of chloride ion position with respect to the BA*n* ring.

fore, modified barbituric acid molecules are able to form four stable complexes with chloride. Through the C–H activated bond (C–H···Cl$^-$), through the ring plane (π···Cl$^-$), through the R$_1$ main group (C–R$_1$···Cl$^-$), and through the N–H bond (N–H···Cl$^-$). Figure 3 shows the molecular graphs of optimized complexes (molecular graphs of N–H···Cl$^-$ complexes are shown in Figure S2, and molecular structures in water are shown in Figure S3). The methylene group is able to moves out of the ring plane to interact with the anion (Figure 1), adopting an axial position. This group has also enough mobility to let the chloride interacts with the most positive part of the ring (see electrostatic potential of **1** in Figure 2). Then, when chloride approaches through the other face of the ring in order to interact with the R$_1$ group, the BA*n* molecule adopts almost the same structure as that in the first case (C–H···Cl$^-$ interaction).

In the gas phase, the most thermodynamically preferred coordination site is the N–H group, as shown in Figure 4 (see
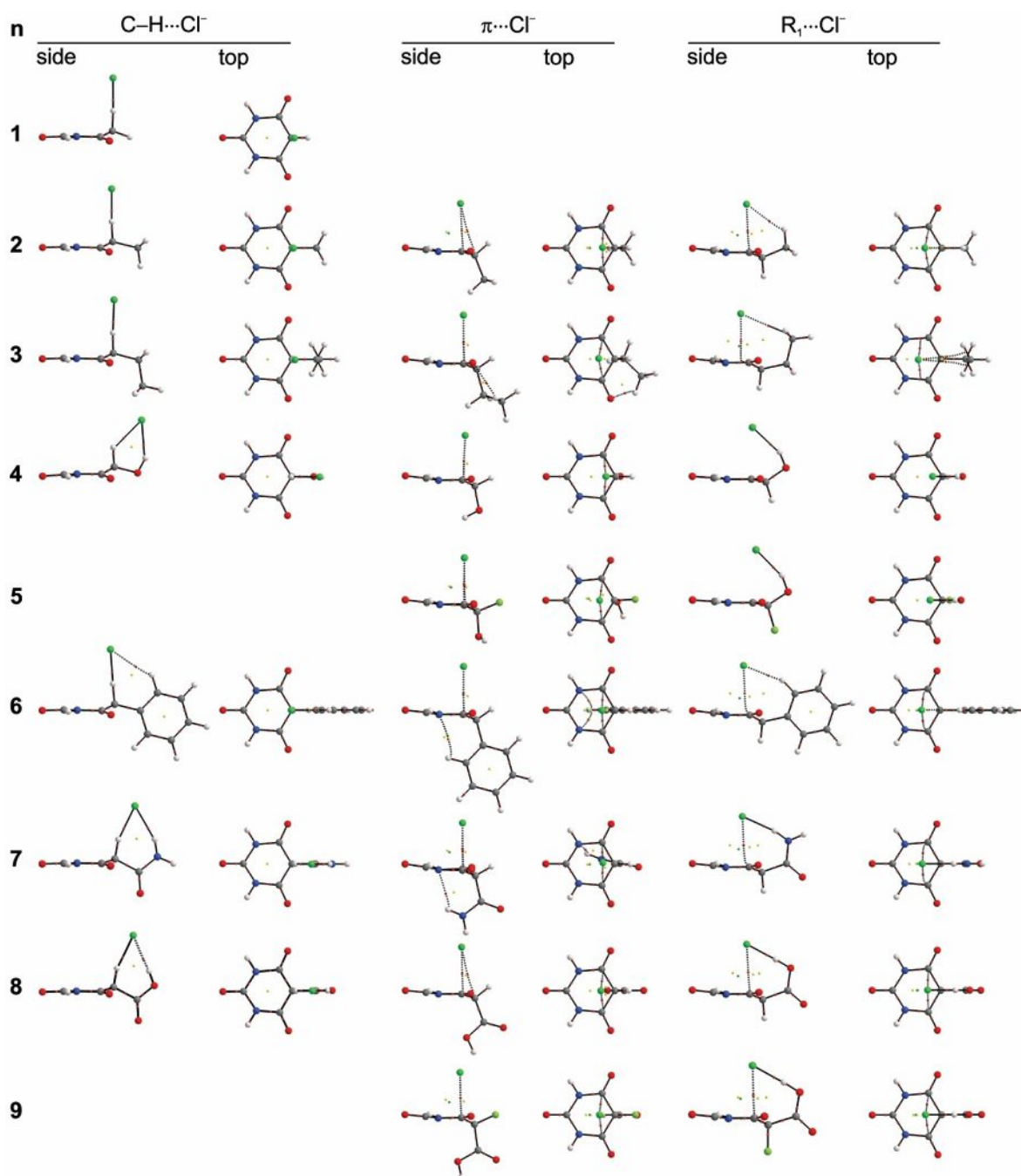
ChemPhysChem

Articles
doi.org/10.1002/cphc.202100008

Chemistry
Europe
European Chemical
Societies Publishing

Figure 3. Top and side views of molecular graphs of BAn@Cl⁻ (n = 1–9) complexes.

Gibbs free bonding energies ΔG_{bond}), followed by the C–H bond. Either in gas phase or in water, the strongest bonding energies are those for BA7, BA8 and BA9. In water, the most favored interactions are C–H···Cl⁻ and C–R₁···Cl⁻. It is worth mentioning that the thermodynamic preferences of N–H···Cl⁻ interactions over C–H···Cl⁻ ones (or other type of configuration) may change in different solvents, as was experimentally demonstrated by Gale and co-workers.[39]

2.3. Topological Analysis

The four types of anionic interactions that barbiturates can form have distinctive topological features (see Figure 3 and Figure S2). In general, the C–H···Cl⁻ hydrogen bond shows angles near 180°, except when the R₁ groups are –OH, –NH₂ or –COOH. The N–H···Cl⁻ hydrogen bonds also show angles near 180°, except in the BA6@Cl⁻ complex (see Figure S2). We summarize the local topological properties of C–H···Cl⁻ and N–H···Cl⁻ hydrogen bonds in Tables 2 and 3. The properties
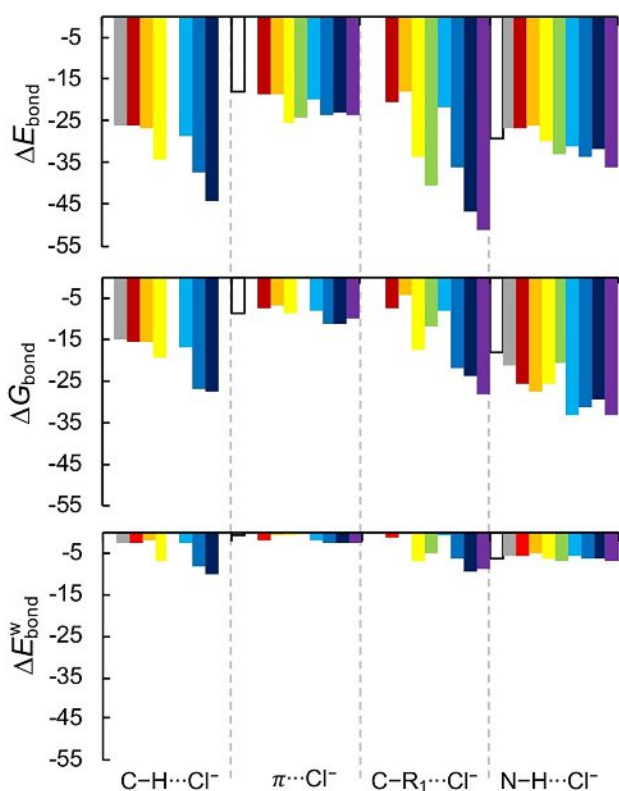
Figure 4. Analysis of the bonding energies of barbiturate@chloride complexes in the gas phase (bonding ΔE_{bond}, and Gibbs free energies of bonding ΔG_{bond}) and in water (ΔE_{bond}^{w}). See full analysis in the Supporting Information (Table S4).

reported in these tables are the electron density, ρ, the Laplacian of the electron density, $\Delta^2\rho$, the total energy density, H, the ellipticity, ε, and the delocalization index, $\delta(H,Cl^-)$.

At the $H\cdots Cl^-$ intermolecular bond critical points, as can be seen in Tables 2 and 3, the purely $C-H\cdots Cl^-$ hydrogen bonds show lower values of ρ than the $N-H\cdots Cl^-$ ones, but they have comparable covalent characters, that is, similar values of H and $\delta(H,Cl^-)$. The charge density ρ values of the $C-H\cdots Cl^-$ interactions within our $BAn@Cl^-$ complexes are larger than those reported for the same interactions in ionic liquids, such as choline@Cl$^{-[7]}$ and 1-ethyl-3-methylimidazolium@Cl$^{-[40]}$ com-

plexes. In addition, according to the total energy densities, our systems also show a greater covalent character for the same interactions. The bond ellipticity ε gives information about the charge accumulation within the plane around the bond path and is also a measured of the bond instability when ε takes high values.[41] If we compare the pure $C-H\cdots Cl^-$ and $N-H\cdots Cl^-$ hydrogen bonds, the former shows ellipticities near zero (around 0.001) and the later show values near 0.011, see for instance complexes $BA1@Cl^-$, $BA2@Cl^-$ and $BA3@Cl^-$. When other interactions take place, beside the $C-H\cdots Cl^-$ one, the coordination strength of the $C-H$ bond decreases, and this is reflected on the local properties. For example, the covalent character of the $C-H\cdots Cl^-$ hydrogen bond decreases in complexes $BA4@Cl^-$ to $BA8@Cl^-$, while the structural instability increases. Nevertheless, the overall coordination strength is superior for complexes $BA7@Cl^-$ and $BA8@Cl^-$, as shown by the bonding energies in gas phase and in water. These results indicate that if we rationally keep the angle $C-H\cdots Cl^-$ within 180° in the presence of a second interaction with chloride, the overall coordination energy should rise even more. We have addressed this situation by replacing the amide group ($-CONH_2$) in $BA7@Cl^-$ by an acetamide ($-CH_2CONH_2$) one (Figure S4). Indeed, this modification improves the coordination energy by 2.4 kcal mol^{-1}, being the highest one among all the complexes. However, there is an energy penalty related to the deformation energy, because the acetamide group has more degrees of freedom.

With regards to the $\pi\cdots Cl^-$ type of complexes, all of them displays bond critical points between the chloride ion and the C atoms of the carbonyl group (see top views in Figure 2). There are only two cases in which a third bond critical point appears between the chloride ion and the sp^3 C5 of the methylene group, in line with previous $C=O\cdots C(sp^3)$ tetrel bonds.[19] The reported values, which are summarized in Table S5, are characteristic of weak closed-shell interactions: low values of ρ, positive laplacian $\Delta^2\rho$, and $H\approx 0$.

Finally, when chloride interacts with the R_1 group through the other face of the barbiturate, the topology is similar as that on the $\pi\cdots Cl^-$ type of complexes. The local properties are reported in Table S6 in the Supporting Information. The R_1 groups coordinate the anion and, at the same time, there are $C\cdots Cl^-$ bond critical points indicating there is a contribution of

Table 2. Values of local topological properties (a.u.) at the $H\cdots Cl^-$ bond critical points for $BAn@Cl^-$ ($n=1-9$) complexes corresponding to the $C-H\cdots Cl^-$ configuration.[a]

Complex	Interaction	ρ	$\Delta^2\rho$	H	ε	$\delta(H,Cl^-)$
$BA1@Cl^-$	$C-H\cdots Cl^-$	0.051	0.064	−0.011	0.002	0.269
$BA2@Cl^-$	$C-H\cdots Cl^-$	0.051	0.066	−0.011	0.001	0.266
$BA3@Cl^-$	$C-H\cdots Cl^-$	0.053	0.065	−0.012	0.001	0.271
$BA4@Cl^-$	$C-H\cdots Cl^-$	0.025	0.066	0.001	0.069	0.152
	$O-H\cdots Cl^-$	0.028	0.065	−0.001	0.018	0.130
$BA6@Cl^-$	$C-H\cdots Cl^-$	0.009	0.028	0.001	0.336	0.065
	$C-H\cdots Cl^-$	0.048	0.069	−0.009	0.001	0.246
$BA7@Cl^-$	$N-H\cdots Cl^-$	0.026	0.065	0.000	0.010	0.134
	$C-H\cdots Cl^-$	0.033	0.069	−0.002	0.013	0.186
$BA8@Cl^-$	$O-H\cdots Cl^-$	0.025	0.054	0.000	0.064	0.122
	$C-H\cdots Cl^-$	0.034	0.070	−0.001	0.053	0.204

[a] All values were obtained at B3LYP/6-311++G(d,p).

ChemPhysChem

Articles
doi.org/10.1002/cphc.202100008

Chemistry
Europe
European Chemical
Societies Publishing

Table 3. Values of local topological properties (a.u.) at the H···Cl⁻ bond critical points for BAn@Cl⁻ (n=1–9) complexes corresponding to the N–H···Cl⁻ configuration.[a]

Complex[a]	Interaction	ρ	$\Delta^2\rho$	H	ε	$\delta(H,Cl^-)$
CA@Cl⁻	N–H···Cl⁻	0.061	0.071	−0.014	0.010	0.270
BA1@Cl⁻	N–H···Cl⁻	0.058	0.074	−0.012	0.011	0.261
BA2@Cl⁻	N–H···Cl⁻	0.058	0.075	−0.011	0.011	0.259
BA3@Cl⁻	N–H···Cl⁻	0.058	0.075	−0.011	0.011	0.259
BA4@Cl⁻	N–H···Cl⁻	0.062	0.071	−0.014	0.010	0.272
BA5@Cl⁻	N–H···Cl⁻	0.067	0.063	−0.018	0.009	0.290
BA6@Cl⁻	C–H···Cl⁻	0.009	0.022	0.001	0.121	0.063
	N–H···Cl⁻	0.052	0.081	−0.008	0.022	0.235
BA7@Cl⁻	N–H···Cl⁻	0.065	0.066	−0.017	0.009	0.285
BA8@Cl⁻	N–H···Cl⁻	0.065	0.067	-0.016	0.009	0.282
BA9@Cl⁻	N–H···Cl⁻	0.070	0.059	−0.020	0.008	0.299

[a] All values were obtained at B3LYP/6-311++G(d,p).

the ring. Only complexes BA4@Cl⁻ and BA5@Cl⁻ do not show these types of critical points. When analyzing complexes BA7@Cl⁻ and BA8@Cl⁻, the N–H and O–H bonds of the side chain (amide and carboxylic respectively) are more effective in coordinating the ion than in the C–H···Cl⁻ type of complex. In these C–R₁···Cl⁻ configurations, the N–H···Cl⁻ interaction of the amide group and the O–H···Cl⁻ one of the carboxylic group display more covalent character and higher values of DI(A|B) tan in the C–H···Cl⁻ configuration.

2.4. Energy Decomposition Analysis

We have seen that the bonding energy and the Gibbs free energies of bonding are the most important terms for the stabilization of the complexes. The strength of the coordination is then analyzed by looking at the interaction energies, while its nature is studied through an LMOEDA analysis, as shown in Figure 5.

We can notice that complexes with C–H···Cl⁻ and N–H···Cl⁻ interactions display similar energy components. The covalent contribution is greater than the electrostatic energy. However, the N–H···Cl⁻ interaction in complexes BA7 and BA8 show larger covalent character than that in complexes with C–H···Cl⁻ hydrogen bond. This is due to the presence of N–H···Cl⁻ and O–H···Cl⁻ side interactions that decrease the C–H···Cl⁻ hydrogen bond angle of 180°, as was shown in the previous section. In general, the increase in interaction energy is due to the increase in the orbital interaction. The only exception is BA4@Cl⁻, in which the increase in interaction energy is because of a lowering of the Pauli repulsion and an increase in the electrostatic term.

The systems with π···Cl⁻ interactions show less stabilizing orbital interactions. Despite this term experiences an increment, the interaction energy does not change very much (from −17 to −25 kcal mol⁻¹). An NBO analysis on these systems (see Table S7 in supporting information) shows that the orbital interactions account for charge transfer interactions between chloride lone-pair (LP) orbitals and C=O antibonding acceptor orbitals: $n_{Cl^-} \to \sigma^*_{C=O}$. The second order perturbation energies are also consistent with the ΔE_{pol} values.
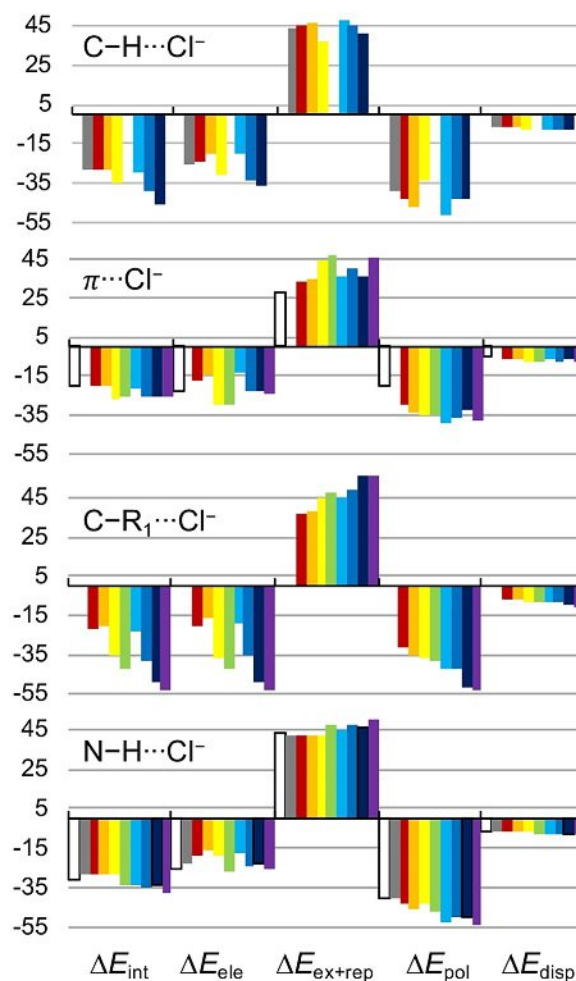

Figure 5. Energy decomposition analysis[a] (kcal mol⁻¹) of optimized structures computed at BLYP-D3(BJ)/aug-cc-pVDZ. CA@Cl⁻ (white), BA1@Cl⁻ (grey), BA2@Cl⁻ (red), BA3@Cl⁻ (orange), BA4@Cl⁻ (yellow), BA5@Cl⁻ (green), BA6@Cl⁻ (light-blue), BA7@Cl⁻ (blue), BA8@Cl⁻ (dark-blue), BA9@Cl⁻ (violet).

On the other hand, the complexes with C–R₁···Cl⁻ interactions show a great augmentation of the interaction energy. It raises from −20.2 in BA2 to −51.1 kcal mol⁻¹ in BA9. This increment is caused by both the orbital and electrostatic energy terms. It has to be noticed that the electrostatic energies follow

ChemPhysChem

Articles
doi.org/10.1002/cphc.202100008

Chemistry
Europe
European Chemical
Societies Publishing

the same trend of the interaction energies. This is because of an exact mutual cancellation of the repulsive ($\Delta E_{exc+rep}$) and attractive ($\Delta E_{pol} + \Delta E_{disp}$) energy terms. It is also worth noting the difference in electrostatic interaction between BA9@Cl⁻ within the π···Cl⁻ and the C–R₁···Cl⁻ type of complex. In these both cases the chloride ion interacts with two different faces of the same ring. As can be seen in Figure S5 (Supporting information) the electrostatic potential of one of the faces is clearly more positive than the other one, therefore it will show a larger electrostatic attraction.

2.5. Designing a Hydrogen-Bonded Receptor

Good and effective anion receptors are usually macrocycles or systems with a certain cavity.[1,4] It is known from a previous work[14] that CA is able to form a hydrogen-bonded quartet with a cage-like structure. Within its cavity, the four CA molecules can hold a NaCl ion pair (see Scheme 3). Due to the similarity of CA with BA1, the latter is expected to form the same type of complex. Therefore, we used this structure as a model system in order to find out whether our modifications on BA1 could improve the coordination strength. By taking into account the strongest interaction energies of all type of coordination
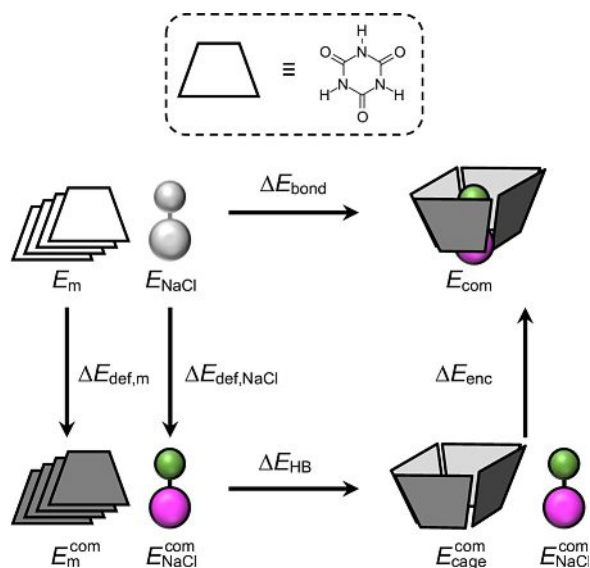
Scheme 3. Partition of the bonding energy and definition of energy terms for the cage-like complexes.

systems (C–H···Cl⁻, π···Cl⁻, C–R₁···Cl⁻, and N–H···Cl⁻), we chose the BA7 and BA9 molecules. As shown in Scheme 3, we partitioned the bonding energy ΔE_{bond} [Eq. (3)] into encapsulation and hydrogen bond energies: ΔE_{enc} and ΔE_{HB} respectively according to [Eqs. (4) and (5)].

$$\Delta E_{bond} = E_{com} - E_m \times 4 - E_{NaCl} \tag{3}$$

$$\Delta E_{enc} = \left(E_{com} - E_{cage}^{com} - E_{NaCl} \right) \tag{4}$$

$$\Delta E_{HB} = \left(E_{cage}^{com} - E_m^{com} \times 4 \right) \tag{5}$$

In these equations, E_{com} is the energy of the coordination complex, E_m is the energy of the isolated monomer and E_{NaCl} is the energy of the isolated ion pair. The super index indicates the structure of the complex.

The overall deformation energy is the sum of the deformation energy of the monomers $\Delta E_{def,m}$ and the deformation energy of the ion pair $\Delta E_{def,NaCl}$, according to Equation (6):

$$\Delta E_{def} = \left[\left(E_m^{com} - E_m \right) \times 4 \right] + \left(E_{NaCl}^{com} - E_{NaCl} \right) \tag{6}$$

If we combined [Eq. (4), (5) and (6)], we will get the overall bonding energy [Eq. (3)]. All interaction energy terms were computed at the BLYP-D3(BJ)/aug-cc-pVDZ level with Counterpoise correction. Table 4 collects all the interaction and deformation energy terms and Figure 6 shows the cage-like complexes.

The coordination complexes of BA1@Cl⁻ have shown a greater coordination capacity than than that of the CA@Cl⁻ complex. In these cage-like complexes, despite BA1 shows no appreciable enhancement of the hydrogen bond and encapsulation energies, the ΔG_{bond} is still more stabilizing than the reference system. The BA9 molecule shows a great deformation energy of the monomers, and a very low hydrogen bond energy (39% lower) with regards to the CA cage. As shown in Figure 7, the congested R₁ groups increase the electrostatic repulsion between the hydrogen bonded monomers. Hence, the overall bonding energy is inferior than that of the CA system. Nevertheless, the coordination energy of the BA9₄ cage is the strongest one among all the systems, which is in line with our previous results.

Our results have shown that the BA9 molecule displays the strongest coordination energy among all the covalent modifica-

Table 4. Values of local topological properties (a.u.) at the H···Cl⁻ bond critical points for BAn@Cl⁻ (n = 1-9) complexes corresponding to the N–H···Cl⁻ configuration.[a]

Complex	$\Delta E_{def,m}$	$\Delta E_{def,NaCl}$	ΔE_{HB}	ΔE_{enc}	ΔE_{bond}
CA₄@NaCl	7.0	−0.3	−47.9	−53.8	−95.0
BA1₄@NaCl	4.8	−0.3	−44.5	−52.3	−92.3
BA9₄@NaCl	41.4	2.6	−29.0	−90.4	−75.4
CA₂BA7₂@NaCl	6.2	1.2	−42.2	−73.7	−108.5
CA₄@NaCl	7.0	−0.3	−47.9	−53.8	−95.0

[a] All values were obtained at BLYP-D3(BJ)/aug-cc-pVDZ

ChemPhysChem

Articles
doi.org/10.1002/cphc.202100008

**Chemistry
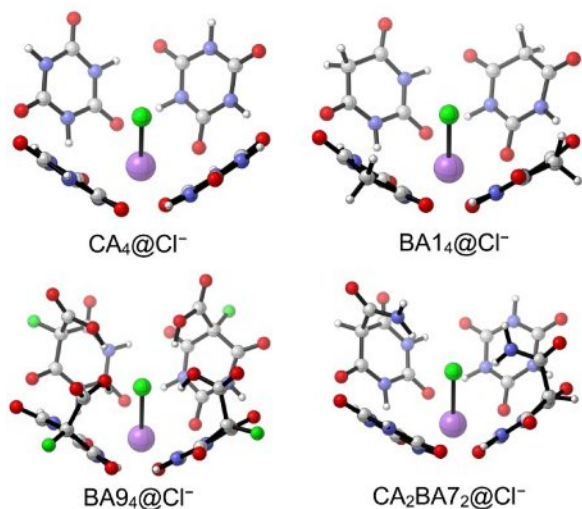Europe**
European Chemical
Societies Publishing

Figure 6. Molecular structures of supramolecular cage-like complexes with NaCl.
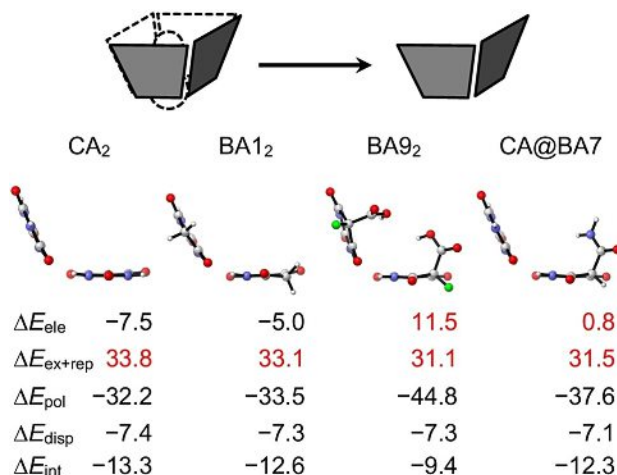

Figure 7. Energy decomposition analysis of hydrogen-bonded dimers within the cage-like complexes. All values were obtained at BLYP-D3(BJ)/aug-cc-pVDZ.

tions. Considering the cage-like complex entirely made of BA9 shows no improvement of bonding energy, we decided to combine two barbiturates with CA. The carboxylic group has a large deformation energy (see Table S4 in supporting information) that decreases the bonding energy; therefore, we selected the BA7 molecule. To this end, we compared the hydrogen bond energies of the homo and heteromolecular dimers; that is CA_2, BAn_2 and $CA@BAn$ dimers (with $n = 1$-9, see deformation, interaction and bonding energies in Tables S7 and S8). Among all these combinations, the $BA7_2$ and $CA@BA7$ dimmers exhibit the lowest deformation energies and the largest bonding energies. Consequently, we built a cage like structure by combining these molecules, as shown in Figure 6. This cage-like structure keeps a hydrogen bonded energy comparable to that of the CA_4 quartet (see also Figure 7), and, at the same time, it owns a higher coordination energy.

Summing up, we were able to gradually improve the coordination strenght of a model receptor in a rational way. According to the Gibbs free energies of bonding, the $CA_2BA7_2@NaCl$ system is the most stabilized. Despite BA is insoluble in water ($1.9 \cdot 10^{-5}$ g/L at $37\,°C$),[42] its hydrophilic character can be improved by adding polar groups into the alkyl substituent.[43] For instance, by adding a nitro group to the C5 position (5-nitrobarbituric acid) the solubility in water rises to 0.9 g/L.[42] In addition, it should be mentioned that BA can undergo solid-state reactions under pressure.[3] As it is mentioned in the introduction, BA can form co-crystals with NaBr, KBr, RbBr, CsBr and CsI by grinding and kneading methods.[18] Even more, BA can also undergo a mechanochemical organic reaction with vanillin after forming a stable co-crystal with the same compound.[44] Therefore, even though the NaCl ion pair complex would not exist in water nor non-polar solvents, it might form co-crystals (under certain conditions) due to the non-covalent interactions studied in our work. We also think BA is a good candidate to be incorporated into other anion receptors.

3. Conclusions

In this work, we have computationally investigated the ability of barbituric acid derivatives to capture chloride anions in gas phase and in water. This ability was shown to be superior to that of cyanuric acid. There are four specific and established ways in which the barbiturates can recognize anions: via the C—H and N—H bonds that act as hydrogen bond donors, through one face of the ring that serves as π receptor and through the other face in which the main R group interacts with the ion. All of these interactions are able to be widely tuned with the covalent modification at position five, being the amide and carboxyl groups the best choices among them all.

Our study shows that the N—H···Cl⁻ interactions are more thermodynamically stabilized than C—H···Cl⁻ ones. However, the smallest difference was found to be 1.4 kcal/mol in gas phase. When looking at the bonding and interaction energies there are some cases in which both interactions have the same values. Therefore, the C—H bond is almost as effective as the N—H bond to recognize chloride ions. We also revealed that the special acidity of the methylene group is due exclusively to a large orbital interaction with the ion, which is not observed in similar environments. The acidity shows up when the C—H bond adopts an axial position. The electrostatic contribution plays a secondary role in the interaction energy. According to the bond descriptors of the QTAIM, both the C—H···Cl⁻ and N—H···Cl⁻ interactions have similar covalence degrees, that is, negative values of the total energy density at the H···Cl⁻ bond critical point and high values of the delocalization index (between 0.2 and 0.3 a.u.). Besides, the coordination capacity of the C—H bond can be enhanced by an additional interaction provided by the functional group at position five. Those groups which have shown the greatest bonding energy in gas phase and in water are the amide (up to −35 and −8 kcal mol⁻¹ respectively) and

ChemPhysChem

Articles
doi.org/10.1002/cphc.202100008

Chemistry Europe
European Chemical
Societies Publishing

the carboxyl groups, (up to -39 and -9 kcal mol^{-1} respectively).

Finally, we have shown how can we use the barbituric interactome in order to improve a potential ionic receptor. Based on a small supramolecular ditopic receptor, we were able to increase its original coordination strength by using one of the most effective barbiturates and keeping, at the same time, a small deformation energy needed for the assembly. Therefore, we think that barbiturates are potentially useful scaffolds to build anionic receptors with different coordinating moieties.

Acknowledgements

Conflict of Interest

The authors declare no conflict of interest.

[1] B. L. Schottel, H. T. Chifotides, K. R. Dunbar, *Chem. Soc. Rev.* **2008**, *37*, 68–83.
[2] P. Ballester, *Chem. Soc. Rev.* **2010**, *39*, 3810–3830.
[3] N. H. Evans, P. D. Beer, *Angew. Chem. Int. Ed.* **2014**, *53*, 11716–11754; *Angew. Chem.* **2014**, *126*, 11908–11948.
[4] J. Zhao, D. Yang, X. J. Yang, B. Wu, *Coord. Chem. Rev.* **2019**, *378*, 415–444.
[5] R. P. Orenha, V. B. Da Silva, G. F. Caramori, F. S. De Souza Schneider, M. J. Piotrowski, J. Contreras-Garcia, C. Cardenas, M. Briese Gonçalves, F. Mendizabal, R. L. T. Parreira, *New J. Chem.* **2020**, *44*, 17831–17839.
[6] R. Plais, G. Gouarin, A. Gaucher, V. Haldys, A. Brosseau, G. Clavier, J. Y. Salpin, D. Prim, *ChemPhysChem* **2020**, *21*, 1249–1257.
[7] C. R. Ashworth, R. P. Matthews, T. Welton, P. A. Hunt, *Phys. Chem. Chem. Phys.* **2016**, *18*, 18145–18160.
[8] H. Juwarker, K. S. Jeong, *Chem. Soc. Rev.* **2010**, *39*, 3664–3674.
[9] Y. Liu, W. Zhao, C.-H. Chen, A. H. Flood, *Science* **2019**, *365*, 159–161.
[10] F. Hettche, P. Reiß, R. W. Hoffmann, *Chem. Eur. J.* **2002**, *8*, 4946–4956.
[11] I. Ravikumar, P. Ghosh, *Chem. Commun.* **2010**, *46*, 6741–6743.
[12] A. Frontera, F. Saczewski, M. Gdaniec, E. Dziemidowicz-Borys, A. Kurland, P. M. Deyà, D. Quiñonero, C. Garau, *Chem. Eur. J.* **2005**, *11*, 6560–6567.
[13] M. Mascal, I. Yakovlev, E. B. Nikitin, J. C. Fettinger, *Angew. Chem. Int. Ed.* **2007**, *46*, 8782–8784; *Angew. Chem.* **2007**, *119*, 8938–8940.
[14] A. N. Petelski, S. C. Pamies, A. G. Sejas, N. M. Peruchena, G. L. Sosa, *Phys. Chem. Chem. Phys.* **2019**, *21*, 8183–8600.
[15] J. T. Bojarski, J. L. Mokrosz, H. J. Bartoń, M. H. Paluchowska, *Adv. Heterocycl. Chem.,*■ **1985**, *38*, 229–297.
[16] K. T. Mahmudov, M. N. Kopylovich, A. M. Maharramov, M. M. Kurbanova, A. V. Gurbanov, A. J. L. Pombeiro, *Coord. Chem. Rev.* **2014**, *265*, 1–37.
[17] G. Mohammadi Ziarani, F. Aleali, N. Lashgari, *RSC Adv.* **2016**, *6*, 50895–50922.
[18] D. Braga, F. Grepioni, L. Maini, S. Prosperi, R. Gobetto, M. R. Chierotti, *Chem. Commun.* **2010**, *46*, 7715–7717.
[19] V. Kumar, P. Scilabra, P. Politzer, G. Terraneo, A. Daolio, F. Fernandez-Palacio, J. S. Murray, G. Resnati, *Cryst. Growth Des.* **2021**, *21*, 642–652.
[20] M. J. Frisch, G. W. Trucks, H. B. Schlegel, G. E. Scuseria, M. A. Robb, J. R. Cheeseman, G. Scalmani, V. Barone, B. Mennucci, G. A. Petersson, H. Nakatsuji, M. Caricato, X. Li, H. P. Hratchian, A. F. Izmaylov, J. Bloino, G. Zheng, J. L. Sonnenberg, M. Hada, M. Ehara, K. Toyota, R. Fukuda, J. Hasegawa, M. Ishida, T. Nakajima, Y. Honda, O. Kitao, H. Nakai, T. Vreven, J. A. Montgomery, Jr., J. E. Peralta, F. Ogliaro, M. Bearpark, J. J. Heyd, E. Brothers, K. N. Kudin, V. N. Staroverov, T. Keith, R. Kobayashi, J. Normand, K. Raghavachari, A. Rendell, J. C. Burant, S. S. Iyengar, J. Tomasi, M. Cossi, N. Rega, J. M. Millam, M. Klene, J. E. Knox, J. B. Cross, V. Bakken, C. Adamo, J. Jaramillo, R. Gomperts, R. E. Stratmann, O. Yazyev, A. J. Austin, R. Cammi, C. Pomelli, J. W. Ochterski, R. L. Martin, K. Morokuma, V. G. Zakrzewski, G. A. Voth, P. Salvador, J. J. Dannenberg, S. Dapprich, A. D. Daniels, O. Farkas, J. B. Foresman, J. V. Ortiz, J. Cioslowski, D. J. Fox, *Gaussian*, Inc., Gaussian 09, Revision D.01, Wallingford CT, **2013**.
[21] A. N. Petelski, C. Fonseca Guerra, *J. Phys. Chem. C* **2019**, *124*, 3352–3363.
[22] S. F. Boys, F. Bernardi, *Mol. Phys.* **1970**, *19*, 553–559.
[23] M. Cossi, G. Scalmani, N. Rega, V. Barone, *J. Chem. Phys.* **2002**, *117*, 43–54.
[24] R. F. W. Bader, *Atoms in Molecules. A Quantum Theory*, Clarendon, Oxford, U. K., **1990**.
[25] T. A. Keith, AIMAll (Version 11.12.19); TK Gristmill Software, Overland Park KS; aim.tkgristmill.com.
[26] P. Su, H. Li, *J. Chem. Phys.* **2009**, *131*, 014102.
[27] M. W. Schmidt, K. K. Baldridge, J. A. Boatz, S. T. Elbert, M. S. Gordon, J. H. Jensen, S. Koseki, N. Matsunaga, K. A. Nguyen, S. Su, T. L. Windus, M. Dupuis, J. A. Montgomery, *J. Comput. Chem.* **1993**, *14*, 1347–1363.
[28] A. E. Reed, L. a Curtiss, F. Weinhold, *Chem. Rev.* **1988**, *88*, 899–926.
[29] G. A. Jeffrey, S. Ghose, J. O. Warwicker, *Acta Crystallogr.* **1961**, *14*, 881–887.
[30] A. M. Pendás, J. L. Casals-Sainz, E. Francisco, *Chem. Eur. J.* **2019**, *25*, 309–314.
[31] S. Nanayakkara, E. Kraka, *Phys. Chem. Chem. Phys.* **2019**, *21*, 15007–15018.
[32] I. Mata, I. Alkorta, E. Espinosa, E. Molins, *Chem. Phys. Lett.* **2011**, *507*, 185–189.
[33] J.-W. Zou, M. Huang, G.-X. Hu, Y.-J. Jiang, *RSC Adv.* **2017**, *7*, 10295–10305.
[34] R. J. Boyd, S. C. Choi, *Chem. Phys. Lett.* **1986**, *129*, 62–65.
[35] G. Buralli, A. Petelski, N. Peruchena, G. Sosa, D. Duarte, *Molecules* **2017**, *22*, 2034.
[36] J. Halldin Stenlid, A. J. Johansson, T. Brinck, *Phys. Chem. Chem. Phys.* **2018**, *20*, 2676–2692.
[37] O. Brea, O. Mó, M. Yáñez, I. Alkorta, J. Elguero, *Chem. Eur. J.* **2015**, *21*, 12676–12682.
[38] G. Caballero-García, G. Mondragón-Solórzano, R. Torres-Cadena, M. Díaz-García, J. Sandoval-Lira, J. Barroso-Flores, *Molecules* **2019**, *24*, 79.
[39] I. E. D. Vega, P. A. Gale, M. E. Light, S. J. Loeb, *Chem. Commun.* **2005**, 4913.
[40] Y. Wang, H. Li, S. Han, *J. Chem. Phys.* **2006**, *124*, 044504.
[41] P. L. A. Popelier, *J. Phys. Chem. A* **1998**, *102*, 1873–1878.
[42] S. L. Yalkowsky, Y. He, P. Jain, *Handbook of Aqueous Solubility Data*, CRC Press, Boca Raton, **2010**, pp. 81, 85.
[43] W. Soine in *Foye's Principles of Medicinal Chemistry*, (Eds.: T. L. Lemke, D. A. Williams.), Lippincott Williams and Wilkins, Baltimore, **2008**, p. 515.
[44] S. Lukin, M. Tireli, I. Loncaric, P. Barisic, D. Sket, D. Vrsaljko, M. di Michiel, J. Plavec, K. Uzarevic, I. Halasz, *Chem. Commun.,*■ **2018**, *54*, 13216.